**An estuarine tuned Quasi-Analytical Algorithm for VIIRS (QAA-V): assessment and application to satellite estimates of SPM in Galveston Bay following Hurricane Harvey**

Ishan D. Joshi[1], Eurico J. D'Sa[1,*]
[1]Department of Oceanography and Coastal Sciences, Louisiana State University, Baton Rouge, LA, USA

Supplementary S1

Chlorophyll-a profiles along with depth-dependent mass-specific IOPs are necessary to create Rrs using Hydrolight® four component case-2 models (Eq.1) (Mobley and Sundman 2013; Sathyendranath et al., 1989; Kirk 1994; Bukata et. al., 1995),

$$a_t(\lambda) = a_w(\lambda) + a_\phi(\lambda) + a_{NAP}(\lambda) + a_g(\lambda)$$
$$b_{bt}(\lambda) = b_{bw}(\lambda) + b_{b\phi}(\lambda) + b_{bNAP}(\lambda) \quad (1)$$

Synthetic chlorophyll concentrations [Chl] (N=730) were obtained with 73 values and ranged between 1 to 40 mg $m^{-3}$ with 10 repetitions to simulate random variability as observed in natural waters. A total of 730 phytoplankton absorption spectra ($a_\phi$) were generated using six groups containing 83 in situ normalized $a_\phi$ spectra; random normalized spectrum selection among groups were based on modeled $a_\phi 440$, and the following bio-optical models (Bricaud et al., 1995; Fischer and Fell 1999; Mobley 1994) (Fig. 1; Table 1),

$$a_\phi^{Normalized}(\lambda) = \frac{a_\phi(\lambda)}{a_\phi 440}$$
$$a_\phi 440 = 0.06 \times [Chl]^{0.65} \times \Re(1,2)$$
$$a_\phi^*(\lambda) = \frac{a_\phi(\lambda)}{[Chl]} \quad (2)$$

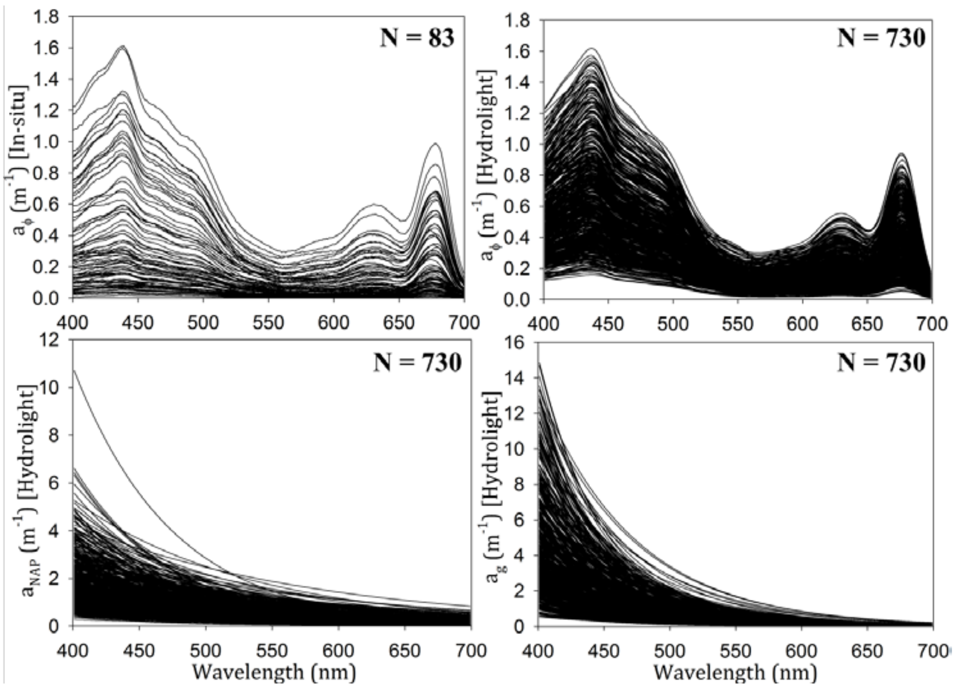


Figure 1. (a, b) *In situ* phytoplankton absorption spectra (N=83) were collected from CDOM-dominated Apalachicola Bay (USA) and sediment-dominated Barataria Bay (USA) to generate 730 simulated spectra for Hydrolight® 4-component Case-2 model using Eq. 2, (c) modeled non-algal particle absorption spectra (N = 730) using Eq. 3, and (d) modeled CDOM absorption spectra (N = 730) using Eq. 4.

Table 1: The conditions for allocating in-situ normalized-phytoplankton spectra ($a_{\phi}^{normalized}$) into 6 groups. $a_{\phi}440$ is phytoplankton absorption at 440 nm.

| Groups (Total spectra = 83) | Condition |
|---|---|
| 1 (n=18) | $a_{\phi}440 < 0.1$ |
| 2 (n=15) | $a_{\phi}440 \geq 0.1$ & $a_{\phi}440 < 0.2$ |
| 3 (n=12) | $a_{\phi}440 \geq 0.2$ & $a_{\phi}440 < 0.3$ |
| 4 (n=11) | $a_{\phi}440 \geq 0.3$ & $a_{\phi}440 < 0.5$ |
| 5 (n=16) | $a_{\phi}440 \geq 0.5$ & $a_{\phi}440 < 1.0$ |
| 6 (n=11) | $a_{\phi}440 \geq 1.0$ |

Mass-specific non-algal particle absorption coefficients ($a_{NAP}^*(\lambda)$) were obtained with an exponential model (Roesler et al. 1989; Bricaud et al. 1995), where slope ($S_{NAP}$) used a random value between 0.005 - 0.015 as observed in natural waters ranging from oceanic to estuarine environments (Kirk 1994). The required $a_{NAP}440$ was modeled using $a_{\phi}440$ based on a constant $p_1$ ($= a_{NAP}440/a_{\phi}440$) which was set to lie between 1 and 3.5 as generally observed in the two bays, e.g., $p_1$ = 1 represents pigment/CDOM-rich waters and $p_1$ = 3.5 represents sediment/CDOM-rich waters (Eq. 3).

$$a_{NAP}(\lambda) = a_{NAP}440 \times e^{-S_{NAP}\times(\lambda-440)}$$
$$p1 = 1 + \frac{2.5\times a_{\phi}440\times\Re(0,1)}{0.05+a_{\phi}440}$$
$$a_{NAP}^*(\lambda) = \frac{a_{\phi}(\lambda)}{[NAP]}$$
$$[NAP] = p1 \times [Chl] \quad (3)$$

CDOM absorption coefficient was modeled with an exponential model (Bricaud et al. 1981), where spectral slope ($S_g$) was chosen randomly between 0.01 to 0.025 as generally observed in various oceanic to productive estuarine environments (Kirk 1994; Babin et al., 2003) (Figure 1d). $a_g440$ was estimated from $a_{\phi}440$ and a constant p2 (= $a_g440$ /$a_{\phi}440$). $p_2$ was set between 1 to 4.5 based on field data, e.g., $p_2$= 1 represents phytoplankton/sediment dominated waters and $p_2$ = 4.5 represents CDOM-rich waters (Eq. 4).

$$a_g(\lambda) = a_g440 \times e^{-S_g\times(\lambda-440)}$$
$$a_g440 = p2 \times a_{\phi}440$$
$$p2 = 1 + \frac{3.5\times a_{\phi}440\times\Re(0,1)}{0.02+a_{\phi}440}$$
$$a_g^*(\lambda) = \frac{a_g(\lambda)}{[Chl]} \quad (4)$$

Mass-specific phytoplankton backscattering ($b_{b\phi}^*$) and non-algal particle back-scattering ($b_{bNAP}^*$) coefficients were obtained based on the oceanic models (IOCCG 2006; please see references therein) with no change, as insufficient observations were available for estuarine environments. Subsequently, these coefficients were then converted to respective back-scattering coefficients by multiplying phase function dependent values “0.005” and “0.0183” (Eqs. 5 and 6) (Mobley 1994; Mobley and Sundman 2013),

$$b_{bNAP}^*(\lambda) = \frac{b_{NAP}(\lambda)\times 0.0183}{[NAP]} \quad (5)$$
$$b_{b\phi}^*(\lambda) = \frac{b_{\phi}(\lambda)\times 0.005}{[Chl]} \quad (6)$$

Hydrolight® simulations were then run with a case-2 model to generate Rrs using mass-specific IOPs, chlorophyll concentrations, dark bottom sediments, finite depth of 5 meters, sun zenith angle of 30$^{o}$, no Raman scattering, and no chlorophyll fluorescence. A total of 169 erroneous spectra were suspected possibly due to atypical combinations of CDOM, non-algal particles, and bottom reflectance; these were not used in further analysis.

References

*IOCCG (2006). Remote Sensing of Inherent Optical Properties: Fundamentals, Tests of Algorithms, and Applications. Lee, Z.-P. (ed.), Reports of the International Ocean-Colour Coordinating Group, No. 5, IOCCG, Dartmouth, Canada.*

IOCCG report 5. http://www.ioccg.org/groups/lee_data.pdf

Supplementary S2

Table 2: Comparison statistics between the QAA-V and QAA-v6 algorithms based on simulated Hydrolight® dataset (HL) and in-situ estuarine and near-shore dataset (IES). N= number of observations, RMSE=Root mean square error, MRE= mean relative error.

| | N | $Bias_{log10}$ ($m^{-1}$) | | $RMSE_{log10}$ ($m^{-1}$) | | MRE (%) | | $R^2$ | |
|---|---|---|---|---|---|---|---|---|---|
| | | QAA-V | QAA-v6 | QAA-V | QAA-v6 | QAA-V | QAA-v6 | QAA-V | QAA-v6 |
| **Synthetic data** | | | | | | | | | |
| $a_{tnw}$**411** | 561 | -0.028 | -0.088 | 0.074 | 0.117 | 12.7 | 19.7 | 0.92 | 0.92 |
| $a_{tnw}$**443** | 561 | -0.006 | -0.071 | 0.071 | 0.106 | 12.7 | 17.7 | 0.91 | 0.90 |
| $a_{tnw}$**489** | 561 | -0.003 | -0.076 | 0.072 | 0.110 | 13.0 | 18.0 | 0.91 | 0.89 |
| $a_{tnw}$**555** | 561 | -0.020 | -0.118 | 0.096 | 0.149 | 16.3 | 23.9 | 0.87 | 0.87 |
| $b_{btnw}$**411** | 561 | -0.041 | -0.159 | 0.097 | 0.173 | 15.5 | 28.9 | 0.95 | 0.95 |
| $b_{btnw}$**443** | 561 | -0.025 | -0.130 | 0.086 | 0.152 | 14.4 | 25.3 | 0.95 | 0.94 |
| $b_{btnw}$**489** | 561 | -0.017 | -0.119 | 0.082 | 0.146 | 14.1 | 23.9 | 0.95 | 0.94 |
| $b_{btnw}$**555** | 561 | -0.018 | -0.121 | 0.089 | 0.153 | 14.9 | 23.9 | 0.94 | 0.93 |
| **IES dataset (Testing set: N = 219)** | | | | | | | | | |
| $a_{tnw}$**443** | 209 | -0.023 | -0.091 | 0.142 | 0.180 | 22.7 | 25.8 | 0.83 | 0.76 |
| $a_{tnw}$**555** | 209 | -0.029 | -0.124 | 0.190 | 0.249 | 34.3 | 47.5 | 0.72 | 0.63 |
| $b_{btnw}$**532** | 89 | 0.038 | -0.049 | 0.173 | 0.174 | 26.0 | 34.6 | 0.70 | 0.67 |

Supplementary S3

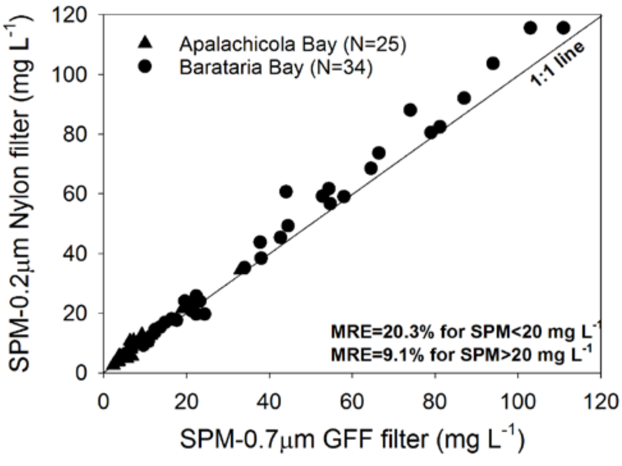


Figure 2: A comparison of SPM concentration obtained with 0.2 µm Nylon filter and 0.7 µm GFF filters.